The Scientific Journal of University of Benghazi

http://journals.uob.edu.ly/sjuob

# Comparison of Computational and Previous Experimental Studies on Naphthyl Pyridyl Pyrazole (NPP)

Othman O. Dakhil [1*] , Maraia F. Elmhdwi [1], Mohamed J. Elarfi [1], Hussniyia A. Al-Difar[1]

*1 Department Chemistry, faculty of science, University of Benghazi, Benghazi-Libya.*

Received 15 / 04 / 2022; Accepted 26 / 06 / 2022

**الملخص**

أجريت دراسة نظرية لجزيء نافثيل بإيرادين بايرازول (NPP). دعمت البيانات التي تم تحديدها من خلال حسابات من نتائج تجريبية من تقنيات الرنين المغناطيسي واشعة اكس. كما حدد التركيب الهندسي والطاقات المثلى للجزيء من خلال نظرية الكثافة الوظيفية (DFT) على المستوى النظري B3LYP 6-311 ++ G. كما تم الحصول على أطياف الاهتزازات وتعيين الاهتزازات الأساسية، وسجلت التحولات الكيميائية للطيف المغناطيسي باستخدام طريقة المدار الذري غير المتغير(GIAO). علاوة على ذلك، حددت الخصائص الإلكترونية، مثل طاقات HOMO وLUMO من خلال النظرية الوظيفية للكثافة المعتمدة على الوقت (TD-DFT). بالإضافة لذلك عثر على نتائج الحسابات لتكون قابلة للمقارنة مع النتائج التجريبية التي تم الحصول عليها.

**الكلمات المفتاحية:** نافثيل بإيرادين بايرازول، تقنيات الرنين المغناطيسي، النظرية الوظيفية للكثافة.

**Abstract**

The naphthyl pyridyl pyrazole (NPP) was the subject of a theoretical inquiry. The data determined through the calculations were supported by experimental results from 1HNMR and X-Ray techniques. Geometrical parameters and optimized energies for the NPP molecule were determined via density functional theory (DFT) at the B3LYP 6-311++G (d, p) level of theory. The vibrational spectra were obtained and the fundamental vibrations were assigned. 1HNMR chemical shifts were recorded by using the gauge-invariant atomic orbital (GIAO) method. Further, electronic properties such as HOMO and LUMO energies were determined via time-dependent density functional theory (TD-DFT). The results of the calculations were found to be comparable to the experimental results obtained.

**Keywords:** DFT, naphthyl pyridyl pyrazole (NPP), HOMO and LUMO.

## 1. INTRODUCTION

Pyrazoles[1] and their derivatives have attractive biological, physiochemical and photochemical properties. They have a number of very important pharmaceutical applications.[2,5] Whilst pyrazoles exist in nature, they are generally obtained via a number of well-established synthesis procedures[5]. They are also utilized as a multi-dentate ligand based on bis and more 3-(2-pyridyl)pyrazole arms in coordination chemistry[5,8]. The main feature of pyrazoles is their highly conjugated system. This property has been used in many studies for the quantitative and qualitative analysis of pyrazole derivatives.[8]

UV-visible spectroscopy is characteristically used in analytical chemistry for such highly conjugated organic compounds. The solvent used directly affects the absorption patterns seen in UV/Vis spectroscopy. Some polar solvents, such as methanol, can form hydrogen bonds with the organic molecule under analysis, which results in blue and red shifts in the peaks compared with nonpolar solvents[9,13]. Numerous studies are available on the relationship between UV absorption frequencies and the solvent used [14].

The aims of this study are (1) to determine various physical properties of (NPP) using DFT, (2) to calculate the HOMO and LUMO energies of NPP in different solvents, and (3) to determine theoretical UV-Vis and $^1$H NMR properties of NPP and (4) to give a comparison of the theoretical and the experimental results so determined [1] (Figure 1).

*__Correspondence__: Othman O. Dakhil
*othmandakeel@yahoo.com*

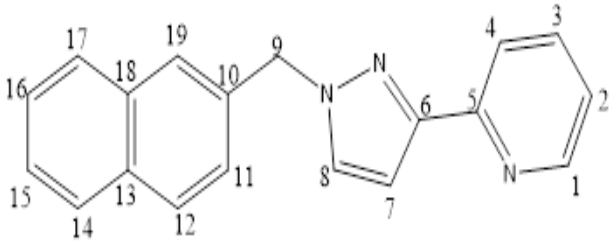



**Figure 1. The general structure of 1-[(2-naphthyl) methyl]-3-(2-pyridyl)-1*H*pyrazole (NPP).**

## 2. COMPUTATIONAL METHODS

The experimental UV and 1H NMR spectra of NPP were obtained from a previous study.[1] Theoretical calculations were undertaken utilizing the Gaussian 09 suite of program codes.[15] Geometric, vibration, magnetic resonance analysis, atomic charges, dipole moment and thermodynamic properties were presented herein. The density functional theory (DFT)[16] approach was chosen to use the Becke three-parameter hybrid functional (B3)[17,18] for the exchange part of the potential in combination with the Lee–Yang–Parr (LYP) correlation functional [19] due to its cost-effective approach and its great accuracy in experimental values.

The time-dependent (TD-DFT) method [20,21] with the same basis set utilized to calculate various electronic properties (UV/Vis spectra, excitation energies, etc. The GIAO method[22,23] is one of the most common approaches for the determination of nuclear magnetic shielding properties.

©2022 University of Benghazi. All rights reserved. ISSN:Online 2790-1637, Print 2790-1629; National Library of Libya, Legal number : 154/2018

Therefore, 1H NMR isotropic chemical calculations were obtained via the GIAO method based on the optimized ground state structure.

## 3. RESULTS AND DISCUSSION

The studying molecule has three moieties naphthalene, pyrazole and pyridine. The calculations were performed in C1 symmetry group (**Table 1**).

**Table 1. The calculated energy and thermodynamically various parameters for NPP at 298.15 K in neutral ground state at the B3LYP/6-311++G (d, p) level of theory**

| Parameters | C1 symmetry |
|---|---|
| Energy (RB3LYP) | -892.35949478au |
| Sum of electronic and thermal Energies= | -892.017777 |
| Sum of electronic and thermal Enthalpies= | -892.003448 |
| Sum of electronic and thermal Free Energies= | -892.002504 |
| Dipole moment (Debye) | 1.6174 |

## 4. Geometrical Structures

The crystal structure of the NPP is given in the literature[6]. Optimized geometric structural parameters were compared with this structure. The optimized structure of the NPP molecule was given with the names and numbers of atoms (Figure 2). The optimized parameters found for this molecule are listed in **Table 2**, based on the numbers scheme given in **Figure 2**.

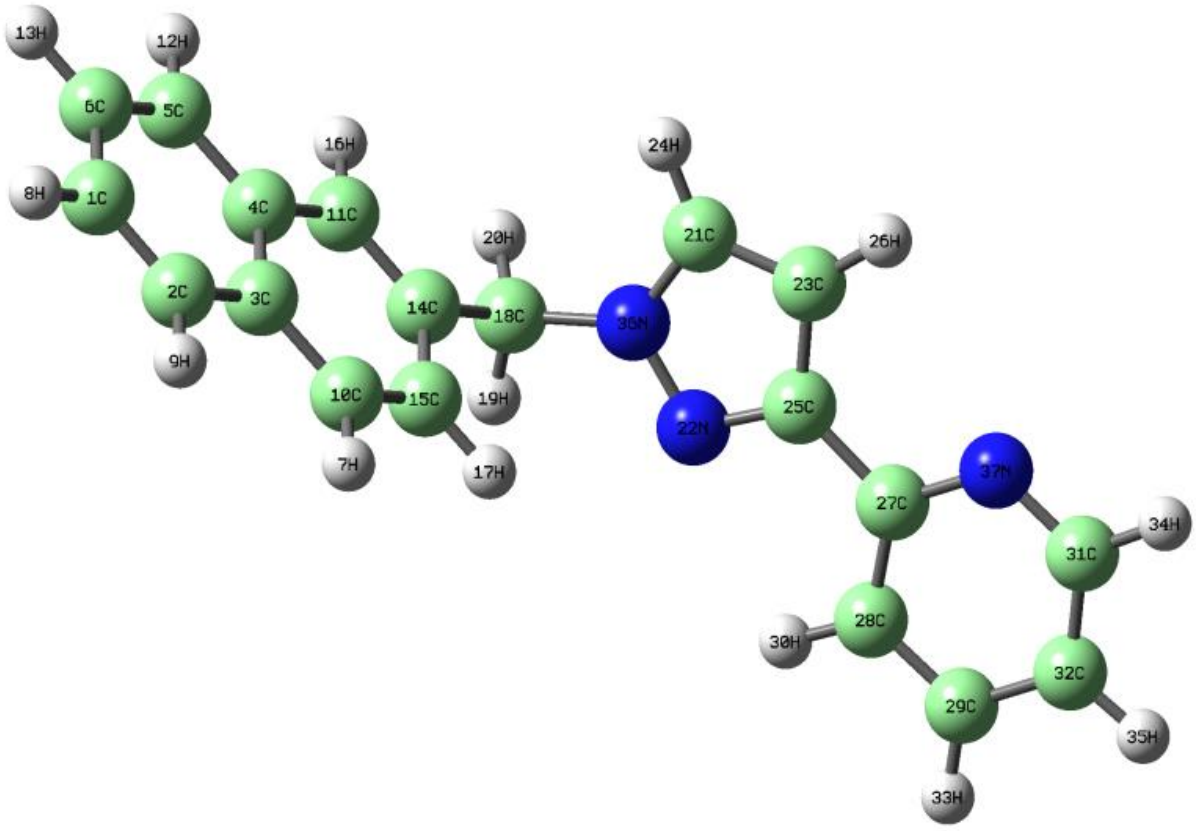



**Figure 2. The optimized structure of NPP**

©2022 University of Benghazi. All rights reserved. ISSN:Online 2790-1637, Print 2790-1629; National Library of Libya, Legal number : 154/2018

**Table2.The experimental and theoretical bond lengths (Å) and bond angles (°) of NPP molecule as determined via B3LYP/6-311++G (d, p).**

| Bond (A°) | Experimental | Calculated NPP | Angle(°A) | Experimental | Calculated NPP |
|---|---|---|---|---|---|
| $N_{36}$—$C_{18}$ | 1.350(2) | 1.466 | C21 —N36 —C18 | 128.52(16) | 119.901 |
| $N_{22}$ —$N_{35}$ | 1.353(2) | 1.396 | N2 —N36 —C18 | 109.02(18) | 118.701 |
| N36 —C21 | 1.457(2) | 1.375 | C2—C3 —C10 | 122.68(17) | 120.000 |
| C2 —C3 | 1.427(3) | 1.421 | C1 —C2 —C3 | 120.71(18) | 120.000 |
| N37 —C27 | 1.338(2) | 1.352 | C27 —N37 —C31 | 117.35(15) | 121.465 |

Theoretically, the C2—C3 bonds were predicted to be 1.421 Å for NPP. The experimental bond lengths were reported at 1.427Å for NPP as expected, the nitrogen-carbon bonds were shorter than the single carbon-carbon bond. The theoretical bond lengths for N(36) — C(18), N(36) — C(21) and N(37) — C(27) were recorded to be 1.466, 1.375 and 1.352 Å, respectively. The same bonds were determined experimentally to be 1.350, 1.457 and 1.338 Å. Since C(18) is $sp^3$ hybridized, the N(36) — C(18) bond was expected to be the tallest bond. Even though this was corroborated by theory, the experimental bond length here was not the tallest. The central atoms in all the measured angles were $sp^2$ hybridized. All the measured angles should thus all be approximately 120° depending on the various competing steric factors. The experimental and theoretical values were very close to the trigonal planer angle.

A conformational analysis was undertaken to determine the most stable structure of the NPP molecule, the geometry of which is represented in **Figure 3**, while the least stable conformation is represented in **Figure 4**. The difference in the total energies between the most and least stable conformations was 0.050 Ha.

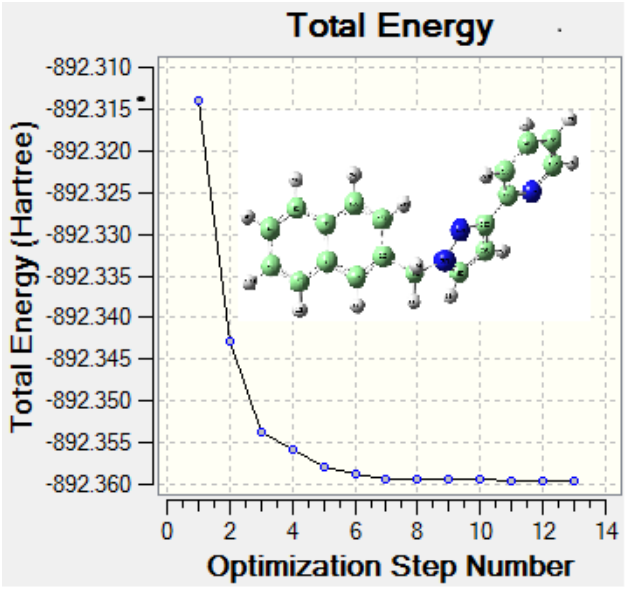



**Figure 3. The most stable structure of NPP**

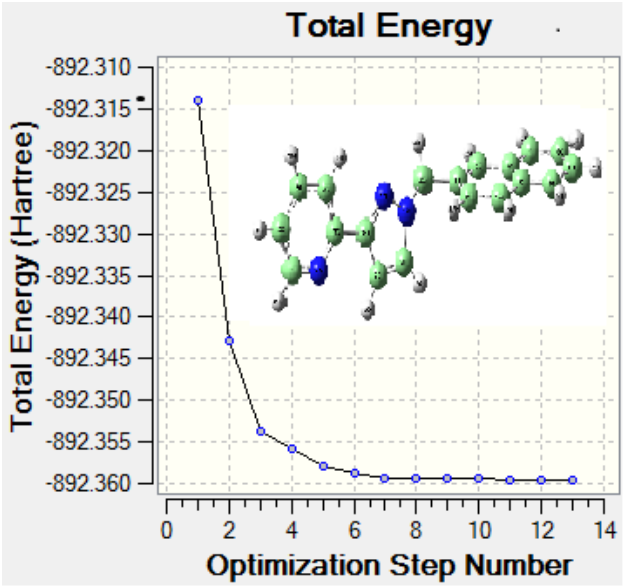



**Figure 4. The least stable structure of NPP**

The lengths of some selected bonds were not in harmony with the molecular stability. As shown in **Figure 5** and **Table 3**, the bond between C(13)—N(36) is the shortest case in conformation 3 (1.443 Å), but it is not the most stable conformation. Similarly, the C(14)—C(19) bond is the shortest in conformation 7 (1.518 Å) as shown in **Figure 6** and **Table 3**.

©2022 University of Benghazi. All rights reserved. ISSN:Online 2790-1637, Print 2790-1629; National Library of Libya, Legal number : 154/2018

**Table 3. The lengths of the C(18)—N(36) and C(14) —C(18) for all NPP optimized structures.**

| | 1 | 2 | 3 | 4 | 5 | 6 | 7 | 8 | 9 | 10 | 11 | 12 | 13 |
|---|---|---|---|---|---|---|---|---|---|---|---|---|---|
| C(18) —N(36) | 1.50 | 1.46 | 1.44 | 1.46 | 1.47 | 1.47 | 1.46 | 1.46 | 1.47 | 1.46 | 1.46 | 1.46 | 1.46 |
| C(14) —C(18) | 1.56 | 1.56 | 1.53 | 1.52 | 1.52 | 1.51 | 1.51 | 1.52 | 1.52 | 1.52 | 1.52 | 1.52 | 1.52 |

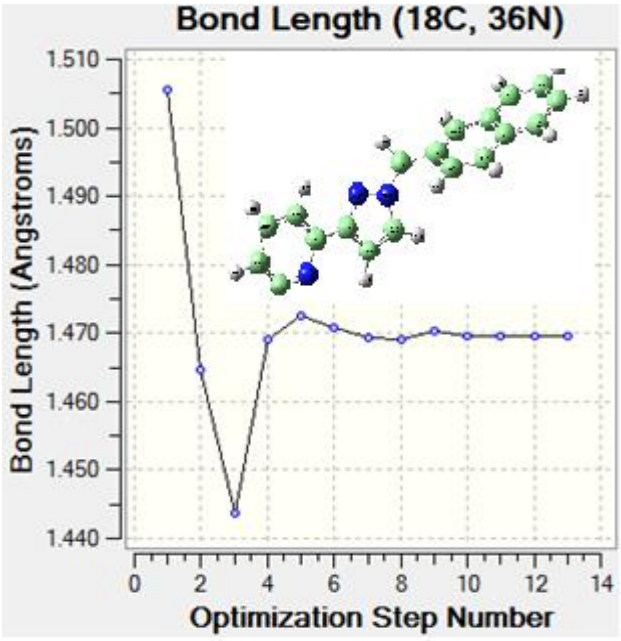



**Figure 5. The length of C(18)—N(36) bond**

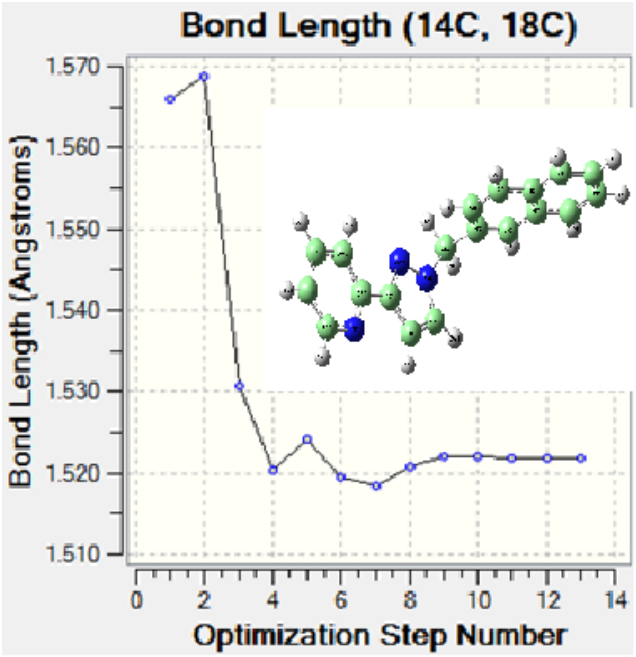



**Figure 6.The length of C(14) —C(18) bond**

Dihedral angles were determined for C(14), C(18), N(22) and N(36). As shown in **Figure 7 a**nd **Table 4**, the dihedral angles decrease with increasing stability of the isomer in question. This relation between dihedral angles and stability broke down for conformation 9. However, at this point, the dihedral increased with decreasing stability. The molecule reached the least dihedral value at conformation10.

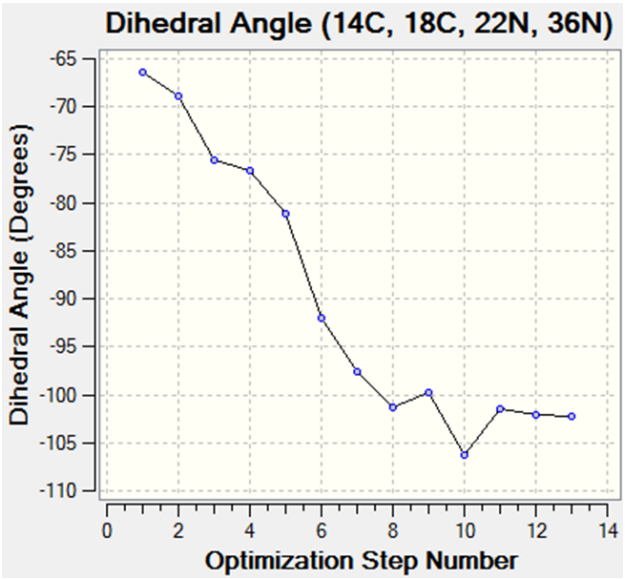
**Table 4. The dihedral angles for (14C, 18C, 22N, 36N)**

| Step No. | Dihedral angle (C14-C18-N22-N36) | Step No. | Dihedral angle (C14-C18-N22-N36) |
|---|---|---|---|
| **1** | -66.463 | **8** | -101.243 |
| **2** | -68.914 | **9** | -99.816 |
| **3** | -75.623 | **10** | -106.259 |
| **4** | -76.708 | **11** | -101.537 |
| **5** | -81.207 | **12** | -102.134 |
| **6** | -92.001 | **13** | -102.276 |
| **7** | -97.599 | | |

**Figure 7. The dihedral angles for (C14-C18-N22-N36)**

**NMR Spectrum Analysis**

$^{1}$H NMR spectra were obtained[6] and predicted. Firstly, full geometry optimization was performed using the gauge-including atomic orbital (GIAO) approach with the DFT/B3LYP method, and 6-311++G(d,p) basis set for chemical shifts predictions. The results of experimental and calculated




NMR spectra are compared in **Table 5** according to the atomic labeling scheme shown in **Figure 1**.

There are two types of hydrogen atoms as in those in the $CH_2$ groups and those on the aromatic rings. The chemical shifts of

©2022 University of Benghazi. All rights reserved. ISSN:Online 2790-1637, Print 2790-1629; National Library of Libya, Legal number : 154/2018

protons of the naphthalene ring H(7), H(8), H(9), H(12), H(13), H(16) and H(17) are predicted theoretically (free molecule) in the range of 6.69–7.04 ppm, while the same protons are predicted theoretically ($CDCl_3$) to be in the range of 6.83–7.25 ppm. The experimental results were recorded at 7.18–7.58 ppm ($CDCl_3$). The $CH_2$ protons group's protons were found to have a theoretical shift of 4.66 H(19) and 4.09(H20) ppm (gas) while in (CDCl3) were 4.51H(19) and 3.87(H20) ppm, respectively. The same protons were recorded experimentally at 5.87 H(19), ($H_20$) ppm. The pyrazole protons, H(24) and H(26) were found to have a theoretical chemical shift of 6.44ppm (gas) and 6.15ppm ($CDCl_3$), and experimentally, were recorded to have a chemical shift of 7.07ppm. The naphthalene protons, H(30) and H(33) were in the range 7.13–7.88 ppm (gas) and 7.05–7.46ppm ($CDCl_3$). Experimentally, they were in the range of 7.07–8.01ppm.

**Table 5. The experimental and theoretical 1H NMR isotropic chemical shifts (with respect to TMS) of the NPP molecule with DFT (B3LYP 6-311++G(d,p)) method**

| Atom | Experimental | Theoretical (ppm) | |
|---|---|---|---|
| | CDCl3 | $CDCl_3$ | GAS |
| H7 | 7.46 | 7.01 | 6.94 |
| H8 | 7.18 | 6.83 | 6.69 |
| H9 | 7.55–7.58 | 7.14 | 6.98 |
| H12 | 7.55-7.58 | 7.25 | 7.04 |
| H13 | 7.23 | 6.95 | 6.72 |
| H16 | 7.45 | 7.01 | 6.89 |
| H17 | 7.45 | 6.94 | 6.73 |
| H19 | 5.87 | 4.66 | 4.51 |
| H20 | 5.87 | 4.09 | 3.87 |
| H24 | 7.07 | 6.77 | 6.54 |
| H26 | 7.07 | 6.44 | 6.15 |
| H30 | 7.94-8.01 | 7.88 | 7.46 |
| H33 | 7.94-8.01 | 7.13 | 7.05 |
| H34 | 8.56 | 8.23 | 7.91 |
| H35 | 6.58 | 6.33 | 6.13 |

### UV-Vis spectrum and molecular orbital investigations

The MO analysis shows the HOMO orbital of the NPP (**Figure 8**). It is mainly localized on the conjugated system (—C=C—) of the naphthalene ring and the lone pair of the pyrroles nitrogen atoms. The LUMO orbitals are more localized on double bonds (—C=C—) of the aryl naphthalene ring and pyridine ring (**Figure 9**). Thus, the charge transfers from the HOMO to LUMO in the compound. NPP is significant due to the contribution of (π) bonds and lone pairs of atoms. **Table 6** shows the energies of the HOMO and LUMO orbitals and the gap between them.

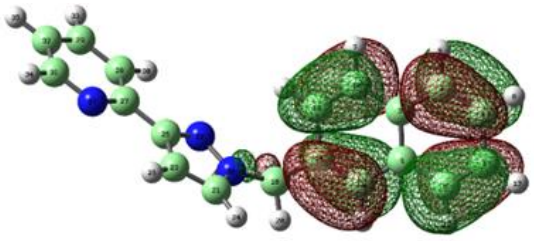


**Figure 8. The HOMO of NPP.**

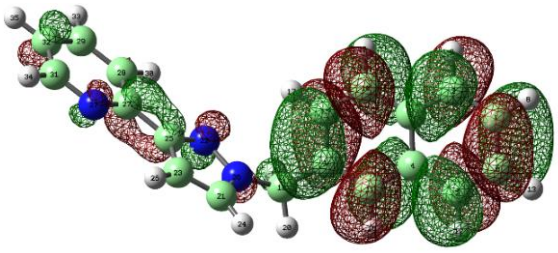


**Figure 9. The LUMO of NPP.**

**Table 6. The energies of HOMO and LUMO.**

| The orbital | Energy |
|---|---|
| HOMO(eV) | 0.29753 |
| LUMO(eV) | 0.09704 |
| GAP(eV) | 0.20049 |

### UV/Vis Spectra

The theoretical UV-Vis spectra and molecular orbital analysis were arranged using the TD–DFT method and the B3LYP/6-311++G(d,p) basis set. The theoretical UV/Vis spectra for the NPP were determined in the gas phase, methanol and dichloromethane are shown in (**Figures 10, 11** and **12** respectively). The calculated absorption (λ), excitation energies (E), and oscillator strength (f) are reported in **Tables 7, 8** and **9** respectively. The peak absorption was recorded at about 260-264nm for all solvents.

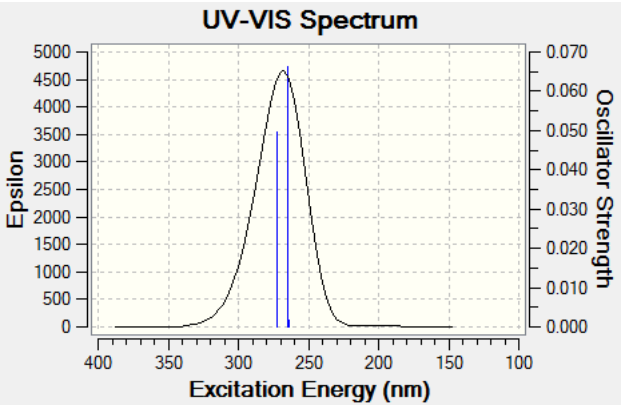



**Figure 10. The UV-VIS spectrum of NPP the gas phase**

©2022 University of Benghazi. All rights reserved. ISSN:Online 2790-1637, Print 2790-1629; National Library of Libya, Legal number : 154/2018

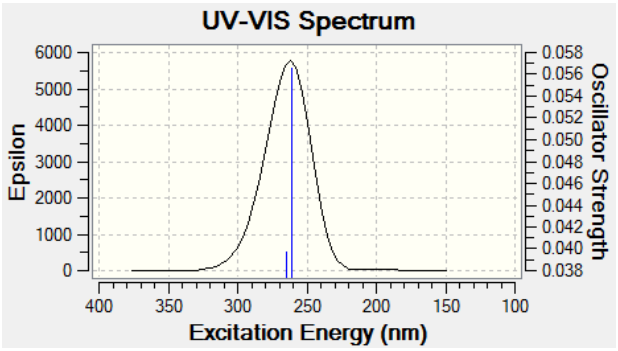



**Figure 11.The UV-VIS spectrum of NPP in $CH_2Cl_2$**

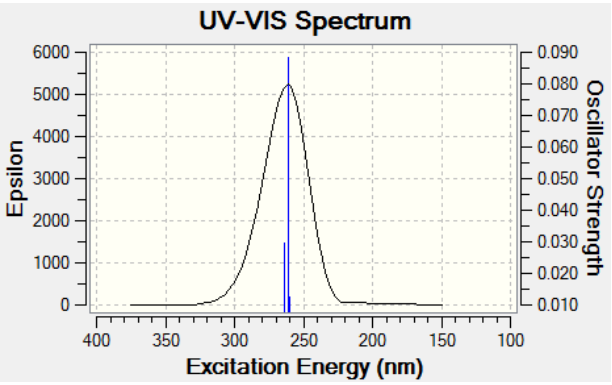



**Figure 12. The UV-VIS spectrum of NPP in methanol**

**Table 7. The calculated absorption wavelengths λ (nm), excitation energies (eV), and oscillator strengths (*f*) of the NPP in the gas phase.**

| Exited state | Wavelength (nm) | Excitation energy(eV) | Configurations composition(corresponding transition orbitals) | Oscillator strength |
|---|---|---|---|---|
| $S_o \rightarrow S_1$ | 272.18 | 4.5552 | 0.18957($H_{-1}\rightarrow L$),0.16774($H_{-3}\rightarrow L$),0.42002($H_{-1}\rightarrow L$), -0.15215($H_{-1}\rightarrow L$-2),0.39241(H →L),0.24764(H →L+2), | 0.0495 |
| $S_o \rightarrow S_2$ | 265.18 | 4.6754 | 0.10510 (H-3 →L), 0.27012 ($H_{-2}\rightarrow L_{-1}$), 0.60837 (H →L) | 0.0663 |
| $S_o \rightarrow S_3$ | 263.43 | 4.7065 | -0.21231 ($H_{-2}\rightarrow L$), 0.60300 ($H_{-2}\rightarrow L_{-1}$), -0.26935 (H →L) | 0.017 |

**Table 8. The calculated absorption wavelengths λ (nm), excitation energies (eV), and oscillator strengths (f) of the NPP in methanol.**

| Exited state | Wavelength (nm) | Excitation energy (eV) | Configurations composition(corresponding transition orbitals) | Oscillator strength |
|---|---|---|---|---|
| $S_o \rightarrow S_1$ | 264.18 | 4.6931 | 0.33829 ($H_{-1}\rightarrow L$), 0.41834($H_{-1}\rightarrow L$), -0.15837(H →L) -0.10249 (H →$L_{-1}$), -0.32111 (H →$L_{-2}$), -0.23032(H→$L_{-3}$) | 0.0295 |
| $S_o \rightarrow S_2$ | 260.89 | 4.7523 | 0.10510 (H-3 →L), 0.27012 ($H_{-2}\rightarrow L_{-1}$), 0.60837 (H →L) | 0.0882 |
| $S_o \rightarrow S_3$ | 260.35 | 4.7621 | -0.21231 ($H_{-2}\rightarrow L$), 0.60300 ($H_{-2}\rightarrow L_{-1}$), -0.26935 (H →L) | 0.0123 |

**Table 9. The calculated absorption wavelengths λ (nm), excitation energies (eV), oscillator strengths (f) pf the NPP in dichloromethane.**

| Exited state | Wavelength (nm) | Excitation energy (eV) | Configurations composition(corresponding transition orbitals) | Oscillator strength |
|---|---|---|---|---|
| $S_o \rightarrow S_1$ | 264.64 | 4.6849 | 0.10388($H_{-1}\rightarrow L$), 0.31584 ($H_{-3}\rightarrow L$), 0.43663 ($H_{-1}\rightarrow L$), -0.19043 (H →$L_{-2}$), -0.35345 (H →$L_{-2}$), -0.12126($H_{-1}\rightarrow L_{-3}$) | 0.0397 |
| $S_o \rightarrow S_2$ | 261.32 | 4.7445 | -0.14674(H-2 →L), 0.48305(H-2 →L-1), 0.45196(H →L), | 0.0566 |
| $S_o \rightarrow S_3$ | 260.94 | 4.7514 | 0.16139 (H-2 →L), -0.45513($H_{-2}\rightarrow$L-1), 0.47728(H →L), | 0.0469 |

©2022 University of Benghazi. All rights reserved. ISSN:Online 2790-1637, Print 2790-1629; National Library of Libya, Legal number : 154/2018

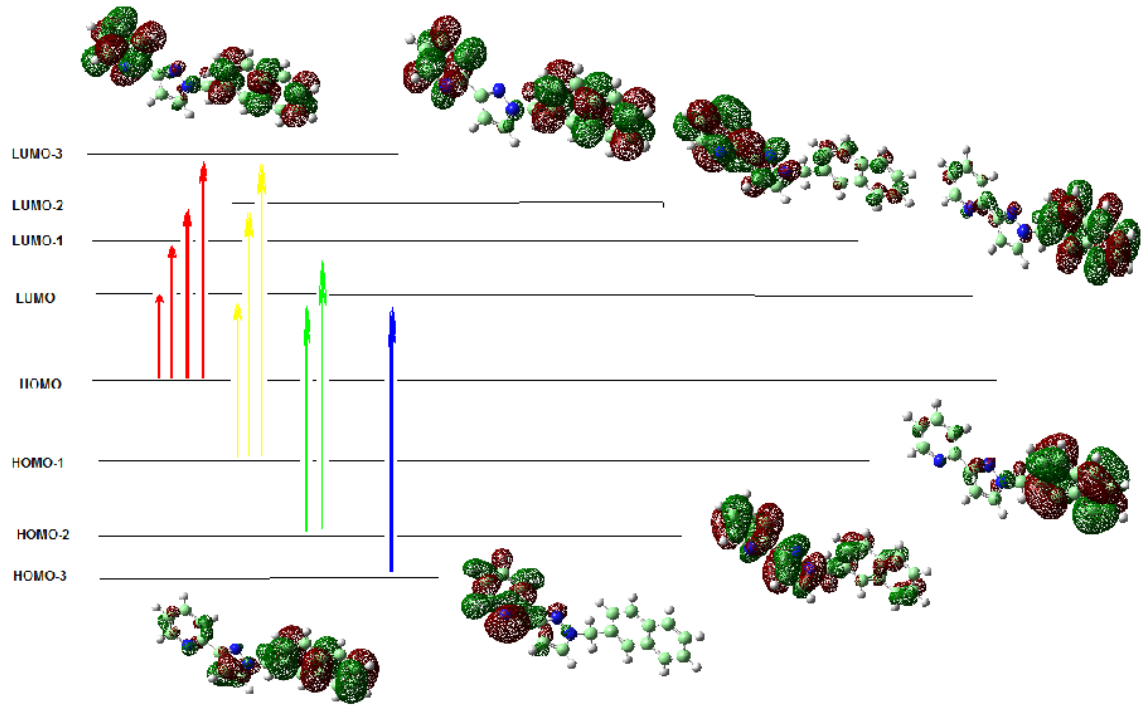



**Figure 13. Form of the MO involved in the formation of the absorption spectrum of NPP at λmax= 263.43as nm calculated at te by B3LYP/6-31G* level of theory.**

## 5. CONCLUSIONS

The study reports an experimental $^{1}$HNMR) and theoretical (DFT) study of NPP. The structure of NPP was fully optimized to determine a stable structure and associated geometric parameters at the B3LYP/6-311++G(d,p) level of theory. The optimized parameters so obtained were compared to those determined experimentally via X-ray spectroscopy. No significant dissimilarities between theory and experiment were observed. There has not been seen big dissimilarity in theory from the experimental values. The 1HNMR spectra were obtained theoretically and compared with the experiment. The theoretical results generally compared well with their NMR data. UV/Vis calculations of gas phase were arranged, methanol and dichloromethane solvents.

## 6. ACKNOWLEDGMENT.

Great thanks to Prof. Mansour H. Almatarneh from the University of Jordan for supporting our efforts with Gaussian 09W and Gauss View.

## 7. REFERENCES

**1.** Biplab D, Sandip S, T.S. Easwari. Asian J. Research Chem. 2012, 5(12).

**2.** Ashraf K, El-dali A, Dakhil O, Alnajar A, Algeriany M. ChemSci Trans., 2014, 3(3).

**3.** Trofimenko S, Scorpionates. The Coordination Chemistry of Polypyrazolylborate Ligands, Imperial College Press, London, 1999.

**4.** Büchel G E, Stepanenko I N, Hejl M, Jakupec M A, Arion V B and Keppler B K. Inorg Chem., 2009, 48, 10737-10747.

**5.** Chi Y and Chou P T. ChemSoc Rev., 2010, 39, 638.

**6.** Najar A M and Ward M D. InorgChem-An Indian, 2013, J., 8(1),11

**7.** Kitagawa S, Kitaura R and Noro S. AngewChemInt Ed., 2004, 43, 2334-2375.

**8.** Zhao X, Xiao B, Fletcher A J, Thomas K M, Bradshaw D and Rosseinsky M. J, Science, 2004, 306, 1012-1015.

**9.** Tong M L, Wu Y M, Ru J, Chen X M, Chang H C and Kitagawa S. Inorg Chem., 2002, 41, 4846-4848.

**10.** Etem KÖSE. The spectroscopic analysis of 2,4'-dibromoacetophenone molecule by using quantum chemical calculations J. of Sci. and Technology – a – Appl. Sci. and Eng. 2016.

**11.** Homocianu M, Airinei A and Dorohoi D O. J Adv Res Phys. 2011, 2(1),1.

**12.** Zakerhamidi M S, Ghanadzadeh A and Moghadam M. Solvent Effects on the UV/ Visible Absorption Spectra of Some Aminoazobenzene Dyes ChemSci Trans.2012, 1(1).

**13.** Geetanj A, and Ram Singh. UV-visible spectral studies on amphiphilic isoalloxazines in single and mixed solvent systems Arch ApplSci Res. 2013, 5(1), 259.

©2022 University of Benghazi. All rights reserved. ISSN:Online 2790-1637, Print 2790-1629; National Library of Libya, Legal number : 154/2018

**14.** Sancho I M, Almandoz M C, Blanco S E and Castro E A. Int J Mol Sci. 2011, 12, 8895-8912.

**15.** Frisch, M. J., Trucks, G.W., Schlegel, H.B., Scuseria, G.E., Robb, M.A., Cheeseman, J.R., et al. Gaussian 09, Gaussian, Inc., Wallingford, CT, 2009.

**16.** Hohenberg, P., Kohn, W. Inhomogeneous Electron Gas, Physical Review. 1964, 136 B864–B871.

**17.** Becke, A.D. Density-functional exchange-energy approximation with correct asymptotic behavior, Physical Review A. 1993, 38, 3098–3100.

**18.** Becke, A.D. Density-functional thermochemistry. III. The role of exact exchange, The Journal of Chemical Physics. 1993, 98, 5648–5652.

**19.** Lee, C., Yang, W., Parr, R.G. Physical Review B. 1988, 37, 785–789.

**20.** Guillaumont, D., Nakamura, S. Calculation of the absorption wavelength of dyes using time-dependent density-functional theory (TD-DFT), Dyes and Pigments. 2000, 46 85–92.

**21.** Fabian, J. TDDFT-calculations of Vis/NIR absorbing compounds, Dyes and Pigments. 2010, 84, 36–53.

**22.** Ditchfield, R. Molecular Orbital Theory of Magnetic Shielding and Magnetic Susceptibility., The Journal of Chemical Physics. 1972, 56, 5688–5691. 17 (4).

**23.** Wolinski, K., Hinton, J.F., Pulay, P. Journal of the American Chemical Society. 1990, 112, 8251–8260.

©2022 University of Benghazi. All rights reserved. ISSN:Online **2790-1637**, Print **2790-1629**; National Library of Libya, Legal number : **154/2018**